

Highlights

Reducing RES Droughts through the integration of wind and Solar PV

Boris Morin, Aina Maimó Far, Damian Flynn, Conor Sweeney

- RES droughts are analysed using 45 years of hourly wind and solar PV generation data
- RES droughts from C3S-Energy and ERA5-Atlite datasets are compared
- Adding solar PV to a wind-dominated system reduces RES drought frequency and duration
- Validated RES datasets are crucial to accurately identify RES drought extremes

Reducing RES Droughts through the integration of wind and Solar PV

Boris Morin^{a,*}, Aina Maimó Far^a, Damian Flynn^b, Conor Sweeney^a

*^aSchool of Mathematics and Statistics, University College Dublin, Belfield, Dublin
4, Dublin, D04 V1W8, Ireland*

*^bSchool of Electrical and Electronic Engineering, University College Dublin, Belfield,
Dublin 4, Dublin, D04 V1W8, Ireland*

*Corresponding author

Email addresses: `boris.morin@ucdconnect.ie` (Boris Morin),
`aina.maimofar@ucd.ie` (Aina Maimó Far), `damian.flynn@ucd.ie` (Damian Flynn),
`conor.sweeney@ucd.ie` (Conor Sweeney)

Abstract

Increasing the share of electricity produced from renewable energy sources (RES), combined with RES dependence on weather, poses a critical challenge for energy systems. This study investigates the importance of the balance between wind and solar photovoltaic (PV) capacity on periods of low renewable generation, known as RES droughts. Three different RES datasets are used to estimate the capacity factors for different scenarios of installed capacities for wind and solar PV power. The skill of the RES models is quantified by comparing capacity factor time series to observed hourly data and by assessing their representation of observed RES droughts. The RES models are used to generate a 45-year hourly time series of RES capacity factor, enabling analysis of the frequency, duration and return periods of RES droughts at a climatological scale. Results show the importance of using an accurate, validated RES model for RES drought risk assessment. The addition of solar PV capacity to a wind-dominated system results in a significant reduction in the frequency and duration of RES droughts, while also reducing extremes and seasonal drought patterns. These findings underscore the importance of diversification in RES capacity to enhance energy security and resilience.

Keywords: RES Drought, Wind Power, Solar PV Power, Renewable Energy Sources, Return Periods

1. Introduction

The EU aims to generate at least 69% of its electricity from renewable energy sources (RES) by 2030, up from 41% in 2022 [1]. While this transition is essential for reducing greenhouse gas emissions, it also highlights the challenge of managing the variability of weather-dependent energy sources such as wind and solar photovoltaic (PV) power. This challenge is amplified by the increasing electrification of energy sectors, which places greater demand on the power system and makes it more sensitive to meteorological conditions, both in historical [2] and future climates [3]. Periods of low renewable generation, known as *Dunkelflaute* or RES droughts, pose significant risks to system adequacy and energy security, emphasising the need for a resilient energy system to meet both growing electricity demand and decarbonisation targets.

RES drought events do not have a fixed definition, with various approaches present in the literature. One common method defines a RES drought as a period during which the average capacity factor (CF) remains below a fixed threshold for a specified duration. For example, Kaspar et al. [4] used this method to investigate the shortfall risks of low wind and solar PV generation in Europe, with a focus on Germany, testing multiple CF thresholds and durations. Similarly, Mockert et al. [5] examined the link between weather regimes and RES droughts in Germany using a 48-hour rolling window under a threshold to define RES droughts. Similar fixed-threshold approaches have also been applied using CF series reconstructed through machine learning in regions such as Japan [6] and Hungary [7].

Alternative methods adjust the CF threshold dynamically over the year to account for seasonal variations in renewable production. Raynaud et al. [8] defined droughts as sequences of days with energy production below a threshold that varies seasonally, a methodology later adapted for India [9]. Building on this, Kapica et al. [10] compared the likelihood of increased RES droughts in Europe under different climate models. Other studies have defined droughts based on deviations from daily mean production: Rinaldi et al. [11] applied these in the U.S. Western Interconnection to quantify the benefits of long-term storage, while Brown et al. [12] examined weekly timescales to explore meteorological influences on the most severe drought events. Another method defines energy drought indices based on metrics commonly used in hydro-meteorology to characterise RES droughts [13]. This approach identifies periods of unusually low generation relative to historical production levels, using the lowest production percentiles. Bracken et al. [14] used this approach to analyse RES droughts at different time scales in the U.S. [14], and Lei et al. [15] used it to quantify droughts in wind-PV-hydro systems in China.

In addition to examining periods of low renewable electricity generation, several studies also explore the periods when the imbalance between renewable generation and electricity demand (residual load) is high. Raynaud et al. [8] defined both energy production and energy supply droughts, and showed the difference in their patterns in a hypothetical fully renewable system composed of wind, PV and run-of-the-river hydropower. Similarly, Allen and Otero [13] also defined a standardised index based on meteorological droughts to address residual load, whose correlation to the energy production index is mostly negative (as expected, although quite low anticorrelations and even small positive correlations appear for some European countries). This

index was also applied to the U.S. by Bracken et al [14], revealing a consistent increase in the drought magnitude when load is considered, despite showing differing results across regions.

In this paper, the focus is exclusively on renewable electricity generation, which allows us to maintain physical models that do not consider the behavioural influence of demand, whose role will be addressed in the discussion. A fixed threshold approach is used to define RES droughts, which facilitates consistent inter-comparison between scenarios with different installed wind and solar PV capacities. The case study used in this paper is Ireland, a region with a strong reliance on wind power and ambitious targets for solar PV power expansion. This provides valuable insights into the potential benefits of diversifying the renewable energy mix on RES droughts in the context of realistic scenarios.

RES droughts are identified using onshore wind and solar PV CF time series. In this study, three different datasets are used and compared, all of which are driven by the ERA5 reanalysis [16]. Two of the datasets are part of C3S Energy (C3SE), an energy-based operational dataset produced by the EU Copernicus Climate Change Service [17]. One of the C3S-E datasets provides CF time series aggregated at the national scale, while the other provides the CF time series at each grid point, at the ERA5 resolution of 0.25° . The third dataset was generated using the Atlite model [18], which converts the ERA5 atmospheric data to a generation time series using specified wind turbine and PV panel models. Atlite is an open-source tool developed by PyPSA [18] and has been used for estimating wind and solar PV generation in order to study RES droughts [5].

Generic datasets for wind and solar PV CF are often used for the quantification of RES droughts. Despite undergoing a validation process, they are often not fully representative of each geographical location, and can show differences in the number of RES drought events [19]. In this work, we quantify the skill of a dataset developed for the European region (C3SE), when used for a specific country (Ireland). In particular, we investigate the impact of a generic versus a tailored dataset on the analysis of RES droughts, in the context of a transition from a wind-dominated system to one with a larger share of solar PV.

The aim of this study is to answer three questions which are relevant for systems with a large share of RES generation:

- Do generic datasets have sufficient skill to reliably quantify extreme

- 89 RES drought events?
- 90 • What is the importance of using accurate RES farm locations, and
 - 91 regionally-validated wind and solar PV models, when analysing of RES
 - 92 droughts?
 - 93 • How does the integration of solar PV into a predominantly wind-based
 - 94 system alter the characteristics of RES drought events?

95 The datasets used in this study are detailed in section 2, which describes
 96 their characteristics and relevance for evaluating RES droughts. Section 3
 97 outlines the RES datasets used to simulate wind and solar PV generation and
 98 provides the methodology for defining and identifying RES drought events,
 99 including the thresholds and metrics applied. In section 4, the datasets are
 100 first verified against observed energy data to assess their accuracy, followed by
 101 an analysis of RES drought occurrences for two scenarios with different ratios
 102 of installed wind to solar PV capacities. Finally, section 5 offers a discussion
 103 of the results in the context of energy reliability and future planning, followed
 104 by the main conclusions and recommendations for further research.

105 **2. Data**

106 This study uses publicly available datasets to construct and validate the
 107 datasets for estimating the CF of wind and solar PV power. The primary
 108 data sources include: EirGrid and SONI, the transmission system operators
 109 (TSO) for the Republic of Ireland and Northern Ireland, respectively; the
 110 ERA5 reanalysis dataset; and the C3S datasets.

111 *2.1. Wind and solar PV Capacity and Availability*

112 EirGrid, the TSO for the Republic of Ireland, and SONI, the Northern
 113 Ireland TSO, provide detailed datasets on all wind and solar PV farms across
 114 the island of Ireland (Republic of Ireland and Northern Ireland) from 1990
 115 to the present [20]. These datasets include information such as each farm’s
 116 installed capacity, name, and connection date. To enhance the accuracy of
 117 this data, the longitude and latitude for each farm were manually determined
 118 through online searches. For simplicity, this data will be referred to as orig-
 119 inating from EirGrid, as all-island data was directly obtained from EirGrid,
 120 and the combined regions of the Republic of Ireland and Northern Ireland
 121 will be referred to as Ireland throughout the remainder of this document.

122 The spreadsheet available from the EirGrid website contains two key vari-
123 ables: generation and availability. Generation is the energy that a RES farm
124 actually contributed to the grid, which may include limitations introduced
125 by the TSO to maintain grid stability, such as constraints and curtailment.
126 Availability represents the energy that would have been generated from a RES
127 farm if no grid constraints had been applied, making it representative of the
128 weather-related response. Generation and availability values are available
129 from 2014 onward for wind power and from 2018 onward for solar PV power,
130 although solar PV availability data only became present in the Republic of
131 Ireland in 2023. This study focuses on availability for all analyses.

132 2.2. Atmospheric Variables

133 All of the datasets used in this study are driven by data from the ERA5 re-
134 analysis [16], produced by the European Centre for Medium-Range Weather
135 Forecasts (ECMWF). This global gridded dataset provides hourly atmo-
136 spheric variables from 1940 to the present at a horizontal resolution of 0.25° .
137 Table 1 lists the relevant ERA5 variables.

Table 1: ERA5 variables used to calculate wind and solar PV generation

ERA5 name	variable
100 metre zonal and meridional wind speed	u_{100}, v_{100}
2 metre temperature	$t2m$
Surface net solar radiation	ssr
Surface solar radiation downwards	$ssrd$
Top of atmosphere incident radiation	$tisr$
Total sky direct solar radiation at surface	$fdir$

138 2.3. C3S Energy

139 The EU Copernicus Climate Change Service developed the C3S-Energy
140 (C3SE) renewable energy dataset for Europe [17], using ERA5 atmospheric
141 variables and weather-to-energy models. This dataset provides hourly CF for
142 wind and solar PV energy from 1979 to the present. The data are available
143 on the same grid as the ERA5 data, which has a horizontal resolution of
144 0.25° . The time series are also available for download at two aggregated
145 scales: regional (NUTS 2) and national.

146 The wind CF in C3SE was calculated using wind speeds at 100 metres
147 (u_{100}, v_{100}) and a standard turbine model, the Vestas V136/3450, with a fixed

148 hub height of 100 meters. As data on wind turbine fleet locations and speci-
 149 fications are difficult to obtain across Europe, C3SE assumes a homogeneous
 150 distribution of wind turbines across the ERA5 grid. While this approach
 151 does not capture the precise capacity factors reported by grid operators, it
 152 provides a well-correlated time series that effectively represents the impact
 153 of climate variability on wind power generation. The C3SE solar PV CF was
 154 also calculated for the ERA5 grid. It is derived from meteorological data, in-
 155 cluding surface solar radiation downwards (*ssrd*) and air temperature (*t2m*),
 156 using a reference solar PV plant model. This model incorporates empirical
 157 calculations for key system components such as optical losses, module effi-
 158 ciency, and inverters. The final CF accounts for a mix of module orientations
 159 typical for each location [21].

160 **3. Methods**

161 This study uses onshore wind and solar PV CF time series from three
 162 datasets to analyse RES droughts across the island of Ireland. Data down-
 163 loaded from C3SE were used to obtain two datasets: one based on national-
 164 level data (C3S NAT), and another on grid-level data (C3S GRD). The third
 165 dataset was computed using the Atlite model (ATL).

166 *3.1. C3S Energy National: C3S NAT*

167 The C3S NAT dataset is created by combining two inputs provided by
 168 C3SE at the corresponding NUTS levels: Republic of Ireland (NUTS0: IE)
 169 and Northern Ireland (NUTS2: UKN0). The two inputs are combined, using
 170 the actual installed capacity as weights. This dataset assumes that RES
 171 generation occurs at every ERA5 grid point in Ireland.

172 *3.2. C3S Energy Gridded: C3S GRID*

173 The C3S GRID dataset uses, as inputs, the actual locations of the RES
 174 farms in Ireland, and the CF from C3SE over the ERA5 grid. For each
 175 farm, the CF from the nearest grid point on the C3SE dataset was selected.
 176 A weighted average of the CF associated with each farm, using the farm's
 177 installed capacities, was used to produce the total CF time series.

178 3.3. *Atlite: ATL*

179 The ATL dataset is produced using the Atlite model. Atlite allows the
180 user to define the wind turbine power curve and PV panel model to use
181 when converting weather variables to wind and solar PV generation. The
182 Atlite model takes as inputs the locations of RES farms and ERA5 weather
183 variables: wind speed at 100 metres (u_{100} , v_{100}) for wind generation, and
184 radiation variables (ssr , $ssrd$, $tisr$, and $fdir$) along with air temperature
185 ($t2m$) for solar PV generation. The output of the Atlite model is a generation
186 time series, which is divided by the total capacity to transform it back into
187 CF. The selection of the wind turbine power curve and PV panel model
188 represents the key difference between this dataset and C3S GRID. This study
189 identifies the most appropriate wind turbine power curve to use from the 121
190 power curves, each at five different levels of smoothing, made available by
191 Renewables.ninja [22], and selects the PV panel model out of the options
192 available within Atlite.

193 3.4. *Energy Scenarios*

194 The datasets provide CF time series for both wind and solar PV. In
195 addition to analysing the CF of wind and solar PV separately, a combined CF
196 was computed for each dataset by averaging wind and solar PV CF, weighted
197 by their installed capacities at the end of 2023 (5.9 GW for wind power and
198 0.6 GW for solar PV power). This configuration is referred to as the 91W-
199 9PV scenario, reflecting the distribution of 91% wind and 9% PV capacity.
200 Given that solar PV capacity in Ireland is low in 2023, and to explore how
201 a more balanced distribution of wind and solar PV capacities might impact
202 RES droughts, this study also considered a second scenario, referred to as
203 57W-43PV, where the installed solar PV capacity is assumed to increase
204 to 8.6 GW, while wind capacity rises to 11.45 GW. These values are based
205 on targets outlined in the roadmap published by the 2024 Climate Action
206 Plan [23]. This study does not include offshore wind in the analysis. Recent
207 reports suggest that even by 2030, Ireland is unlikely to have any significant
208 new offshore wind farms, with projected offshore capacity expected to remain
209 near zero using realistic scenarios [24].

210 New time series were generated for both the ATL and C3S GRD solar
211 PV datasets, incorporating a revised distribution of installed capacity across
212 Ireland as specified in the roadmap. For wind power, the CF time series
213 remains unchanged, as significant shifts in the location of wind farms are not
214 expected. In total, twelve CF time series were analysed in this study, six for

individual wind and solar PV CF (three datasets for each source) in the 91W-9PV scenario, and an additional six time series that include the combined CF for 91W-9PV and 57W-43PV scenarios across the different datasets.

It is important to note that the specific capacity values used in this study are illustrative and are not intended to reflect precise future realities. Instead, they serve to explore the impact of transitioning from a wind-dominated system (91W-9PV) to a more evenly distributed system (57W-43PV). This approach allows for a comparative analysis between the two scenarios, assessing how the balance of RES capacity affects the occurrence of RES droughts.

For each dataset (ATL, C3S GRID, and C3S NAT), four distinct scenarios are examined, as summarised below:

- Wind Power - based on the actual capacity at the end of 2023
- Solar PV Power - based on the actual capacity at the end of 2023
- Combined RES / 91W-9PV - based on the actual capacity at the end of 2023
- Combined RES / 57W-43PV - based on the projected capacity for 2030

3.5. RES Drought Definition

In this study, a RES drought event was defined as occurring when the 24-hour moving average of CF remains below a fixed threshold of 0.1 for a period of longer than 24 hours. By using a 24-hour moving average, fewer but longer-lasting events were captured compared to using the raw CF time series, which can be more sensitive to short-term fluctuations. The 24-hour rolling average also avoids potential masking of day-long events due to their start time. A fixed threshold approach was chosen in this study to enable consistent inter-comparison between datasets.

The moving average approach smooths out short-term fluctuations, so that brief periods above the threshold do not interrupt an otherwise continuous low-CF period (Fig. 1). This means that a single hour above the threshold does not "break" a drought event if it is surrounded by prolonged low-generation hours. As a result, fewer but longer-lasting drought events are identified, which may better reflect real-world conditions where energy supply constraints persist over extended periods.

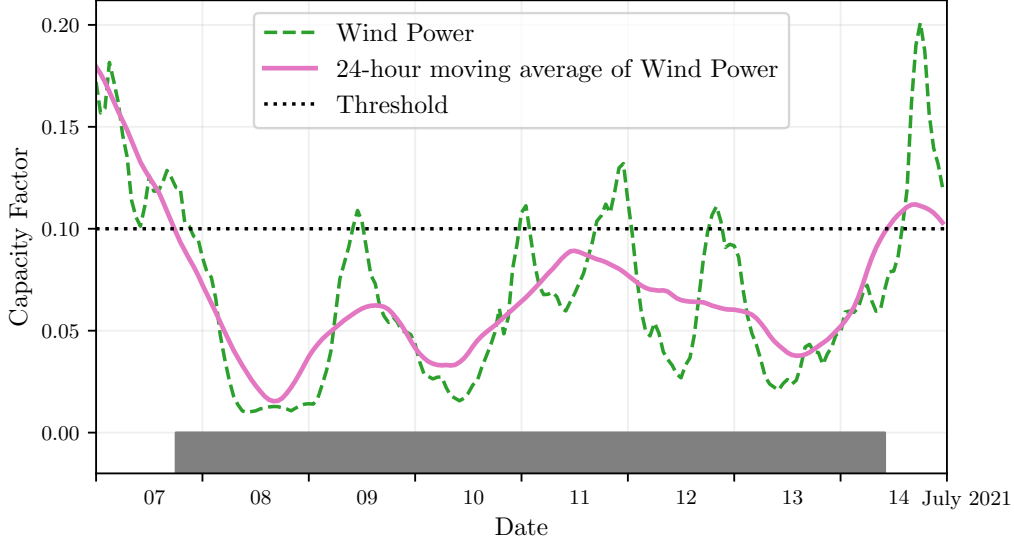


Figure 1: Wind time series of CF (green) and its 24-hour moving average (pink) from the 7th to the 15th of July 2021. The black dashed line indicates the CF threshold. The grey bar shows the period identified as a wind drought under our definition

247 4. Results

248 4.1. Verification

249 The accuracy of the datasets used in this study was verified, before con-
 250 tinuing to the analysis of RES droughts. For the verification process, time-
 251 varying values of installed capacity were used to account for changes in RES
 252 development over the verification period. This step allowed us to assess how
 253 well the datasets represent the production of renewable energy by comparing
 254 them against observed data.

255 4.1.1. Wind Energy

256 The C3S datasets use the Vestas V136/3450 wind turbine power curve
 257 (Fig. 2a). The Atlite model allows the user to specify the power curve.
 258 We considered the 121 power curves available for download from Renew-
 259 ables.ninja [22]. For each power curve, Renewables.ninja also provides four
 260 associated smoothed power curves. The smoothing is done using a Gaussian
 261 filter with different standard deviations that depend on the wind speed. A
 262 separate wind CF time series for Ireland was generated for each of the wind
 263 turbine power curves and smoothing levels.

264 The performance of each CF time series is then assessed based on four skill
 265 scores: correlation coefficient (CC), root mean square error (RMSE), mean
 266 bias error (MBE), and the percentage of overlap. The percentage of overlap
 267 quantifies the similarity between the observed and modelled distributions. It
 268 is a positively oriented skill score, where 100% shows full agreement between
 269 the two distributions, and 0% indicates no overlap. The histograms of hourly
 270 CF values for the most recent decade (2014-2023) are used to calculate this
 271 skill score.

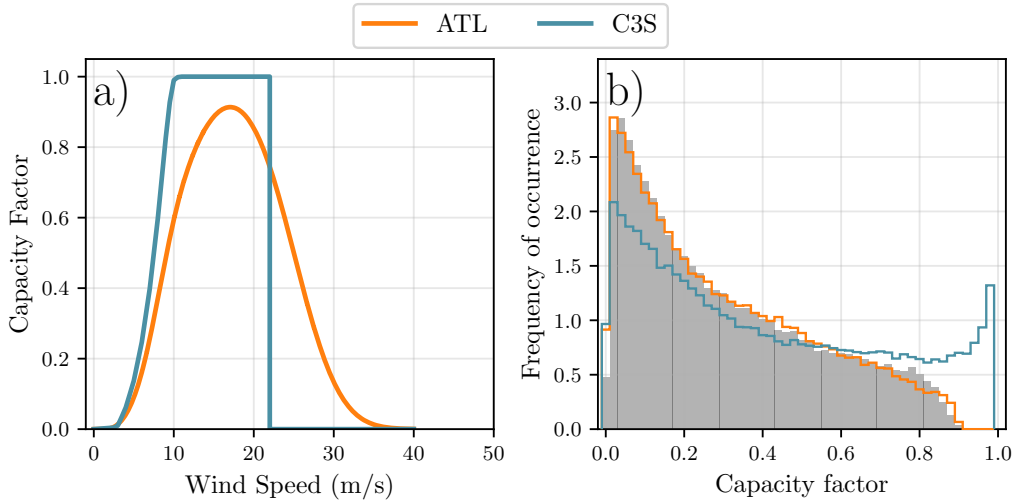


Figure 2: a) Power curves of the Enercon E112.4500 with a $0.3w$ smoothing filter used by ATL (orange) and the Vestas V136/3450 used by C3SE (blue) b) Histograms of wind CF for Ireland from ATL (orange), C3SE (blue) and Observed (shaded)

272 Based on these metrics, the most representative power curve for Ireland
 273 is the Enercon E112.4500 power curve with the $0.3w$ smoothing filter. The
 274 smoothing of the wind turbine power curve represents losses associated with
 275 each turbine, as well as losses such as wake effects between turbines, which
 276 are important when modelling wind energy on larger spatial scales. The
 277 histogram in Fig. 2b shows that the C3SE power curve tends to underestimate
 278 low CF values and overestimate higher ones, whereas the smoothed ATL
 279 power curve more closely follows the observed wind availability data. This
 280 is further supported by the percentage of overlap which is higher for ATL
 281 (97.2%) than for C3SE (83.2%), indicating better agreement with observed
 282 data.

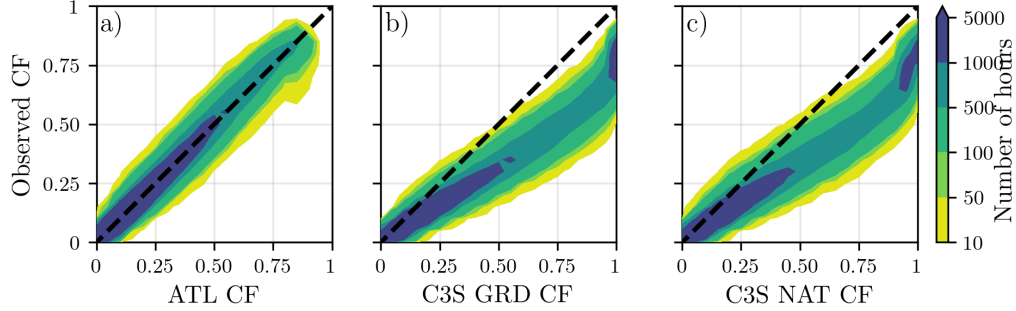


Figure 3: Wind CF density plot of the observed CF (vertical axes) and modelled (horizontal axes) CF data for the a) ATL, b) C3S GRID and c) C3S NAT datasets

283 The effect of the difference between the power curves is also visible in
 284 Fig. 3, which shows a density plot of wind CF values. The two C3S datasets
 285 are shown to overestimate the observed CF, whereas the Atlite model is in
 286 good agreement with the observed data. The skill scores presented in Table 2
 287 show that ATL performs better than the two C3S datasets for all of the skill
 288 scores.

	ATL	C3S GRID	C3S NAT
CC	0.981	0.972	0.970
RMSE	0.045	0.177	0.162
MBE	-0.003	0.137	0.121

Table 2: Skill scores for wind power for the three datasets compared to observed data

289 Fig. 4 shows the average annual number of wind drought events during
 290 the 2014 to 2023 validation period. The figure reveals that ATL presents
 291 the best overall agreement with the observed frequency and duration of wind
 292 drought events. This pattern is particularly evident for shorter-duration
 293 events, which are the most frequent.

294 This verification for wind generation data highlights the importance of
 295 selecting a representative wind turbine power curve for the region being anal-
 296 ysed. The ATL dataset, which uses a representative wind turbine power
 297 curve, is skilled at reproducing wind CF and droughts over Ireland. On the
 298 other hand, the power curve used for both C3S GRID and C3S NAT is not
 299 representative for Ireland, as it severely overestimates generation, underes-
 300 timating the occurrence of RES droughts. This highlights a problem with

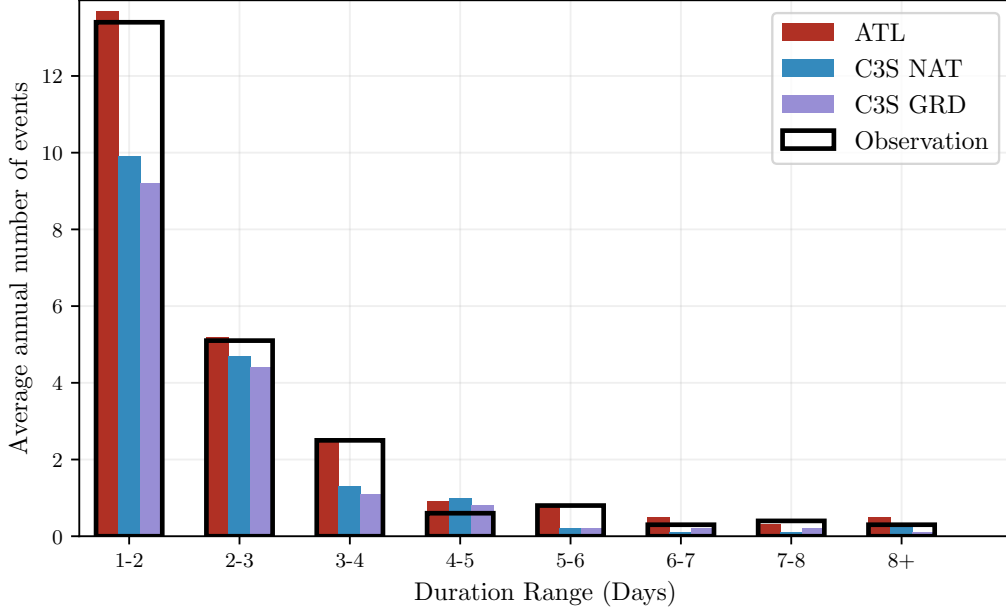


Figure 4: Average annual number of wind drought events for ATL (red), C3S GRD (blue), C3S NAT (purple), and the observed data (black outline). The wind droughts are identified from 2014 to 2023, considering the actual capacity of the system at any given time

301 using generalised datasets for analysing RES droughts: biases severely affect
302 their ability to accurately reproduce RES drought events. The skill scores
303 for the three datasets (Tab. 2) show only a small difference in their ability to
304 reproduce the changes in CF, as seen by their similar CC scores. However,
305 their ability to reproduce the actual CF values is much lower than that of
306 ATL, with RMSE scores almost four times bigger for the two C3S datasets.
307 There is a clear bias towards an overestimation of CF, seen in the MBE
308 values, which leads to the underestimation of droughts. This highlights the
309 need to use regionally verified models to assess RES droughts.

310 4.1.2. Solar PV Energy

311 The Atlite model allows the user to select certain PV panel characteristics.
312 In this study, the three PV panel types available in the Atlite model were
313 considered (CSi, CdTe, Kaneka). Following the same methodology as in the
314 previous section, the three available models were compared using four skill
315 scores (CC, RMSE, MBE, and the percentage of overlap). Based on the best-
316 performing metrics, the Beyer PV panel model was selected [25], using the

317 Kaneka Hybrid panel option. For all solar PV farm locations, the azimuth
318 angle is fixed at 180° (due south), and the optimal tilt angle option is applied.
319 The solar PV installed capacity available on the spreadsheets from Eir-
320 Grid represents the Maximum Export Capacity (MEC) and does not ac-
321 curately reflect the installed solar PV capacity. To enable actual solar PV
322 generation potential to be modelled correctly, installed capacities were set at
323 1.4 times the MEC values. This scaling factor was estimated by analysing
324 proprietary data from individual solar PV farms provided by EirGrid, which
325 showed that, on average, assuming that the installed capacities of farms ex-
326 ceed their MEC values by 40% yields the best agreement with the observed
327 availability.

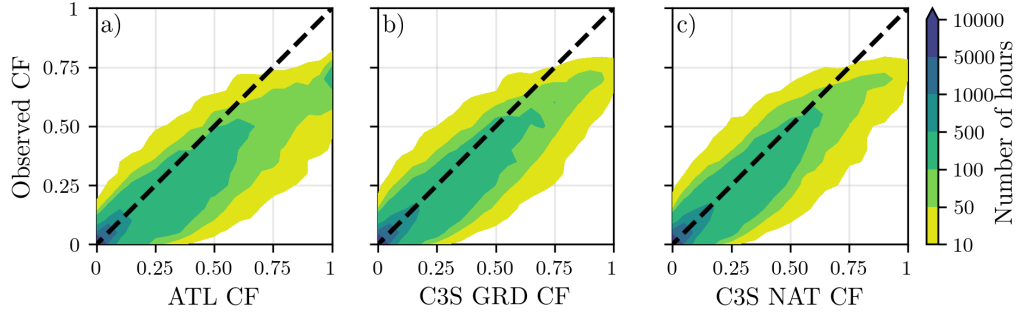


Figure 5: Solar PV CF density plot of the observed (vertical axes) and modelled (horizontal axes) CF series for the a) ATL, b) C3S GRD and c) C3S NAT datasets

328 Figure 5 shows that the three datasets have a similar tendency to over-
329 estimate the CF compared to the observed values, especially for high CF
330 values. The skill scores presented in Table 3 indicate that C3S GRD and
331 C3S NAT perform better than ATL for solar PV CF, with lower RMSE and
332 MBE, and higher CC scores. This may be due to the statistical approach
333 taken by C3SE for the orientation of the PV panels.

	ATL	C3S GRD	C3S NAT
CC	0.921	0.931	0.931
RMSE	0.119	0.090	0.113
MBE	0.046	0.027	0.021

Table 3: Skill scores for Solar PV CF for the three datasets compared to observed data

334 Fig. 6 shows the number of solar PV drought events during the 2023

validation period across different duration ranges. The figure reveals partial agreement between the three datasets and the observed data, with consistent results noticed for duration ranges of 1-2, 3-4, 7-8, and 8+ days. However, discrepancies appear in the other ranges, where the models diverge from the observed data. The main challenge in validating solar PV data stems from the recent installation of a large share of Ireland’s solar PV capacity, with over 65% of the total solar PV capacity installed in 2023. This results in uncertainties in solar PV generation data and the actual generating capacity in the first few months after each farm is connected. Overall, C3S GRD performs slightly better than the other datasets in reproducing observed solar PV drought events.

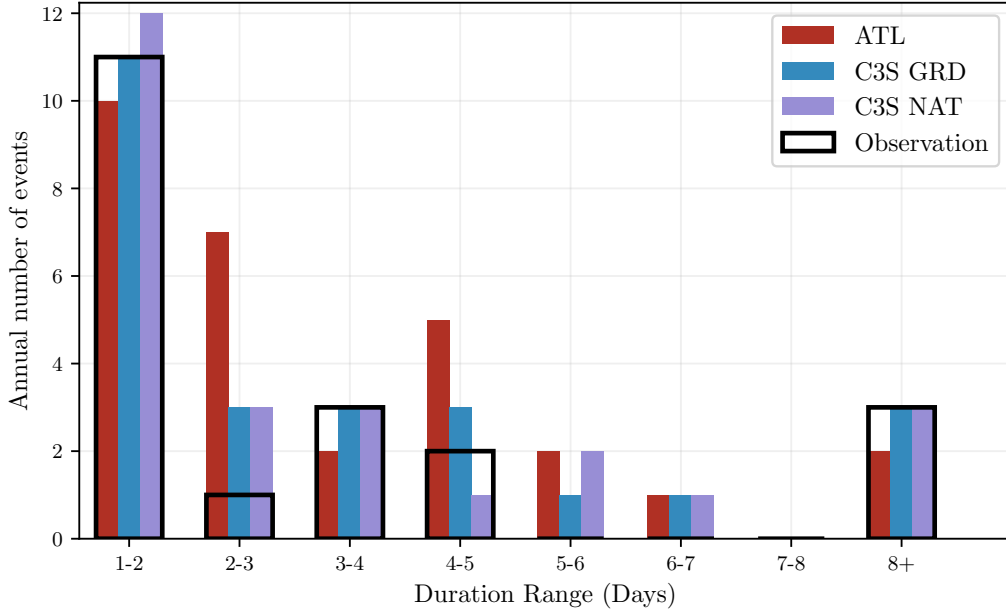


Figure 6: Number of solar PV drought events for ATL (red), C3S GRD (blue), and C3S NAT (purple) and the observed data (black outline). The solar PV droughts are identified for 2023, considering the actual capacity of the system at any given time

4.2. Analysis

In this section, RES droughts are analysed by calculating the frequency and duration of RES drought events, the return periods for different RES

drought durations, and the seasonality of RES drought events. Understanding the characteristics and timing of RES drought events enables system operators to optimally plan for reserve capacity requirements, ensuring grid stability and security of supply. Results are presented for the three datasets, allowing their differences on the characterisation of RES droughts to be clearly identified.

RES drought events are evaluated under two different scenarios with fixed installed capacities: the 91W-9PV scenario, with 5.9 GW of wind capacity and 0.6 GW of solar PV capacity; and the 57W-43PV scenario, where wind capacity comprises 11.45 GW and solar PV capacity increases to 8.6 GW. Both scenarios were driven by 45 years of ERA5 data. Using the RES drought identification process described in Section 3.5, wind and solar PV droughts are first analysed separately before presenting the results for combined (wind + solar PV) RES droughts under both scenarios.

4.2.1. Annual Number of RES Droughts

The first part of the analysis examines the annual number of RES drought events. When only wind energy is considered (Fig.7a), the number of drought events decreases as the duration range increases, with very few events lasting more than seven days. In contrast, for solar PV energy (Fig.7b), drought frequency declines from one to eight days and then slightly increases for longer durations. This behaviour is attributable to Ireland’s high-latitude location, where reduced sunlight in winter (from November to March) leads to consistently low solar PV output.

Moreover, the comparison between wind and solar PV results indicates that the median, first, and third quartiles for solar PV are consistently higher than or equal to those for wind. This is expected, given that solar PV generation is inherently lower, zero at night, and limited by the solar cycle. When wind and solar PV are combined under the 91W-9PV scenario (Fig.7c), the results closely mirror those of wind alone, due to the dominance of wind power in the current energy mix. However, in the 57W-43PV scenario (Fig.7d), a marked reduction in drought events is observed across all datasets, with a decrease of the total number of events of 56% for ATL, 52% for C3S GRD, and 50% for C3S NAT, demonstrating the beneficial effects of a more balanced energy mix.

The consistently higher drought counts reported by the ATL dataset, compared to the C3S datasets, underscore the importance of wind turbine power curve representation when quantifying RES droughts. Whereas the

three datasets agree on the overall effect of balancing the share of wind and solar PV generation, they differ at a quantitative level, which has crucial implications for energy planning.

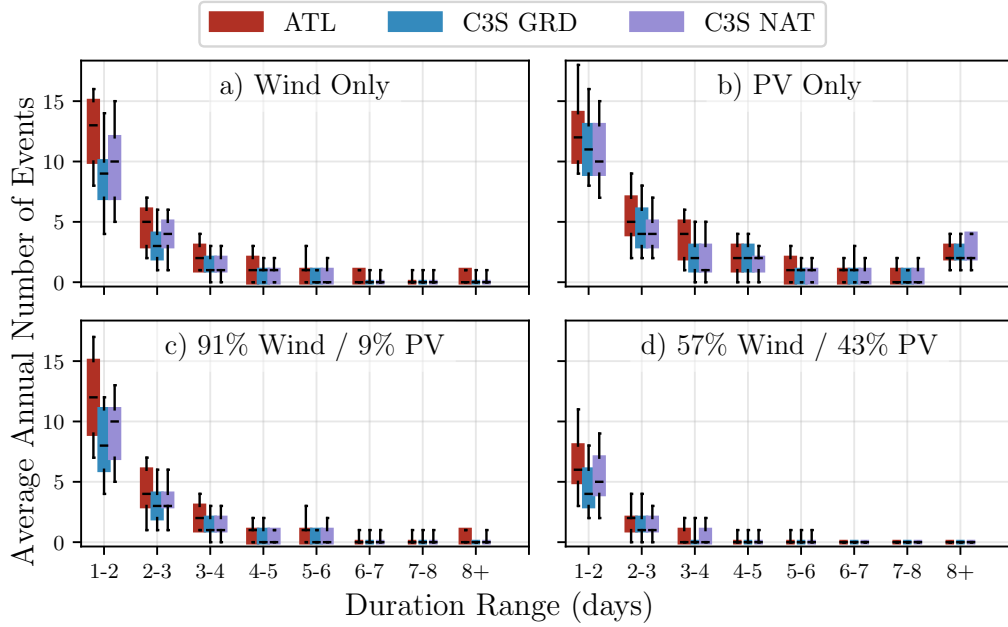


Figure 7: Average annual number of RES droughts (from 1979 to 2023) for a) Wind, b) solar PV, c) 91W-9PV and d) 57W-43PV for ATL (red), C3S GRD (blue), and C3S NAT (purple). The x-axis represents duration ranges in days (lower bound included), while the y-axis indicates the annual number of events. The boxes display the first and third quartiles and the median is marked by a black line. The whiskers indicate the 5th and 95th percentiles

4.2.2. Return Periods of RES Drought Duration

The RES drought events identified over the 45-year period were used to calculate the return periods for different RES drought durations. A return period is the estimated average time interval between events of a specified duration (not to be confused with the frequency of their occurrence within a fixed time frame). Fig. 8 shows the return periods for different RES drought durations, which can be used to capture the most extreme events affecting the system. Understanding their return periods is crucial, as extreme yet rare RES droughts pose the toughest challenge to energy security by placing

398 significant strain on the conventional backup sources necessary to maintain
399 security of supply during these events.

400 For wind (Fig. 8a), the log-linear increase in return periods observed in
401 this study confirms that longer droughts occur exponentially less frequently,
402 a trend consistent with earlier research on wind variability. In the case of
403 solar PV droughts (Fig.8b), the ATL dataset shows a general log-linear trend,
404 whereas the C3S datasets exhibit a sudden increase in drought duration for
405 events exceeding sixteen days. This abrupt rise reflects differences in how
406 solar PV output is handled near the CF threshold during low irradiance
407 conditions.

408 Under the 91W-9PV scenario (Fig. 8c), the combined RES drought return
409 periods mirror those for wind alone, reflecting the dominance of wind in the
410 current energy mix. In contrast, the 57W-43PV scenario (Fig. 8d) shows
411 a dramatic increase in return periods across all durations, suggesting that
412 a more diversified energy mix can substantially mitigate the frequency of
413 prolonged drought events. Despite the lower wind share in the 57W-43PV
414 scenario, typically known for its relative stability, the balanced share with
415 solar PV leads to extended return periods for RES droughts. This result
416 indicates that the complementarity between wind and solar PV plays a crucial
417 role in reducing the occurrence of drought events in a diversified energy
418 portfolio.

419 Across Fig. 8a, c, and, d, the return periods in the ATL dataset are con-
420 sistently higher than those in the two C3S datasets. For instance, in the
421 91W-9PV scenario (Fig. 8c), an event with a one-year return period lasts six
422 days in the ATL dataset, compared to only five days in the C3S datasets.
423 This difference underscores the importance of model selection when quan-
424 tifying RES droughts, as each dataset's assumptions and parametrisations
425 significantly influence drought duration estimates. Additionally, in all four
426 graphs, the similarity between results from the two C3S datasets suggests
427 that assumptions in the ATL dataset, such as wind turbine power curve se-
428 lection and PV panel specifications, have a greater impact on RES drought
429 duration estimates than the precise geographic distribution of RES farms
430 when studying the return periods of RES droughts.

431 The return periods calculated from the three datasets show large differ-
432 ences, in particular for the more extreme events with longer return periods.
433 The C3S datasets produce shorter RES drought durations for these events,
434 which would have the largest impact on the power system. This shows that
435 system planning based on the wrong datasets could yield an underestimation

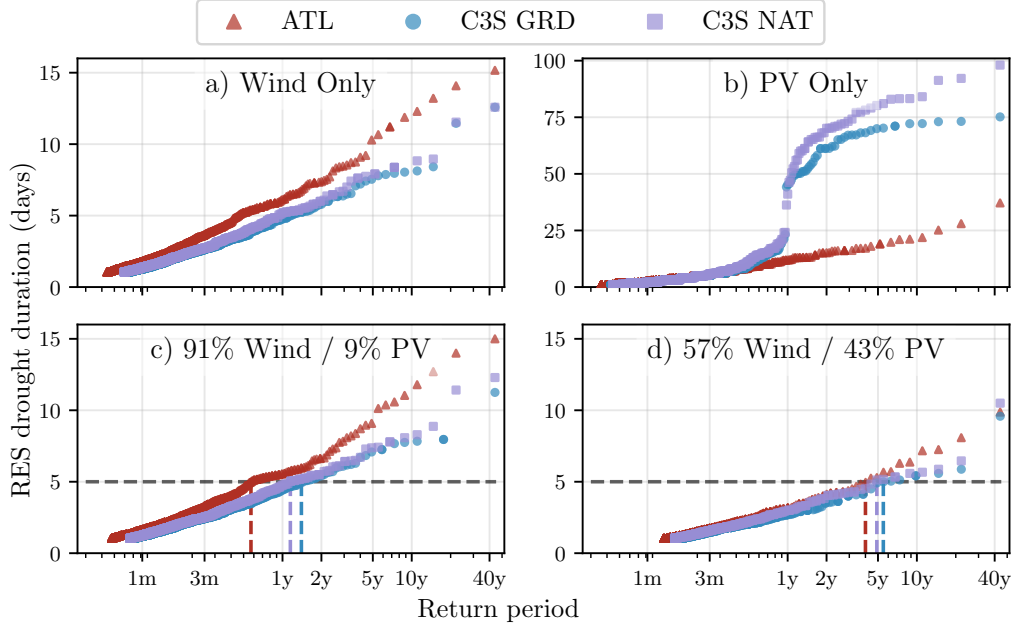


Figure 8: Return periods of the duration of RES droughts (from 1979 to 2023) for a) Wind, b) Solar PV, c) 91W-9PV and d) 57W-43PV for ATL (red triangle), C3S GRD (blue circle), and C3S NAT (purple square). The x-axis represents the return period time in a log-scale and the y-axis indicates the duration of RES drought associated with it. The horizontal dashed line marks the 5-day return period, with coloured vertical dashed marking its return period for each dataset

436 of the duration of extreme RES droughts, potentially leading to shortages
 437 linked to undersized reserve capacity.

438 4.2.3. Seasonal Distribution of RES Droughts

439 The seasonal analysis of RES droughts is based on the percentage of hours
 440 in each month classified as part of a RES drought event. Wind droughts tend
 441 to be more frequent during summer, whereas solar PV droughts are more
 442 common in winter due to reduced sunlight. By comparing these seasonal
 443 patterns across different datasets and energy scenarios, this study examines
 444 how model-specific assumptions and variations in capacity mix affect the
 445 overall characterisation of RES drought events.

446 For the wind-only scenario (Fig. 9a), the ATL dataset exhibits a pro-
 447 nounced seasonal pattern, with about 24% of summer hours (June, July,
 448 August) identified as droughts compared to only 4% in winter (December,

449 January, February). This strong seasonal signal is less evident in the C3S
 450 datasets, which suggests that the differences in the underlying wind power
 451 curves play a significant role. In ATL, CF near or below the 0.1 threshold
 452 occurs at relatively higher wind speeds, resulting in a higher count of drought
 453 hours during the summer months. In contrast, solar PV droughts (Fig. 9b)
 454 display an opposite seasonal trend. Across all datasets, over 60% of winter
 455 hours are classified as solar PV droughts, reflecting the naturally low solar
 456 irradiance in Ireland during winter. Moreover, ATL tends to record a slightly
 457 higher percentage of drought hours for wind and a marginally lower percent-
 458 age for solar PV relative to the C3S datasets. These differences highlight how
 459 dataset-specific assumptions, such as the treatment of wind turbine power
 460 curves and PV panel characteristics, significantly influences the apparent
 461 seasonal dynamics of RES droughts.

462 The 91W-9PV scenario (Fig. 9c) shows patterns comparable to the ones
 463 for wind droughts (Fig. 9a). However, in the 91W/9PV scenario, the number
 464 of hours classified as RES droughts in summer decreases slightly compared to
 465 the wind-only scenario. This reduction can be explained by the contribution
 466 of solar PV generation during the summer months in the 91W-9PV scenario,
 467 even though it constitutes only 11% of total capacity. Since the number of
 468 RES drought hours for solar PV in summer is near zero, this small contribu-
 469 tion has a noticeable impact on reducing overall drought hours. In the 57W-
 470 43PV scenario (Fig. 9d), all three datasets show a reduction in monthly RES
 471 drought frequency. Annual reductions in median RES drought frequency are
 472 observed across the datasets, dropping from 14% to 5% for ATL, from 8%
 473 to 3% for C3S GRD, and from 9% to 4% for C3S-E NAT. The balanced
 474 mix of wind and solar PV power in this scenario reduces the seasonal signal
 475 overall and significantly decreases the percentage of RES drought hours in
 476 the summer.

477 The seasonal variations observed in this study have important implica-
 478 tions for energy planning. Given that energy demand peaks in winter for
 479 Northern European countries, understanding these seasonal patterns is criti-
 480 cal for assessing the need for conventional backup or storage solutions during
 481 periods of prolonged low renewable output. The findings underscore that
 482 even small differences in model assumptions leads to significant variations in
 483 drought estimates, thereby affecting the reliability of the energy system dur-
 484 ing critical periods. Additionally, the integration of large shares of solar PV
 485 in the system leads to a general reduction of RES droughts year-round. How-
 486 ever, it can not counter the presence of RES droughts in the winter months

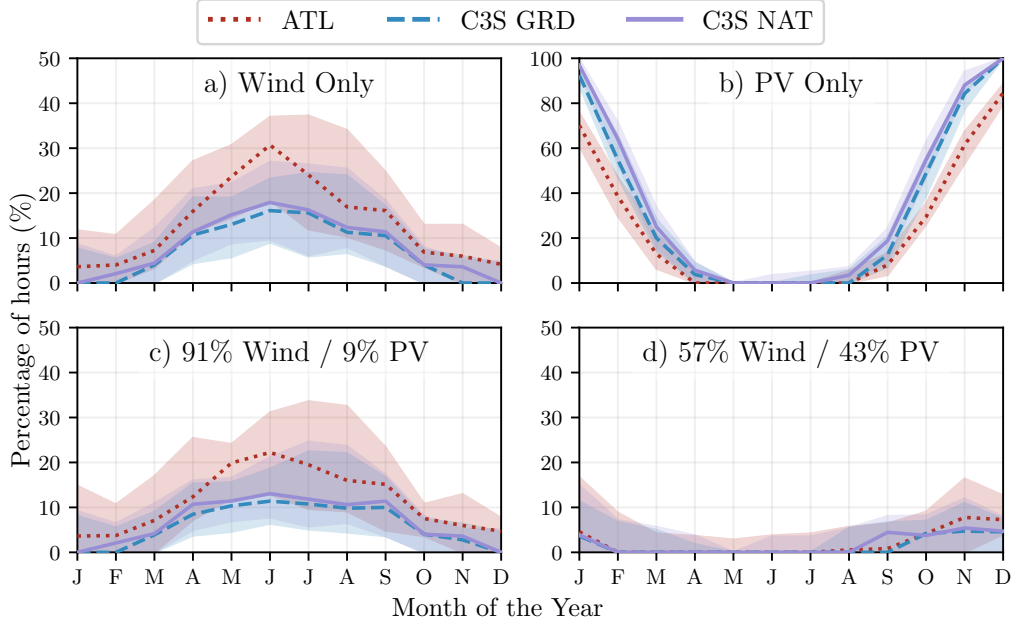


Figure 9: Percentage of hours in a month which are part of a RES drought (from 1979 to 2023) for a) Wind, b) Solar PV, c) 91W-9PV and d) 57W-43PV for ATL (red dotted), C3S GRD (blue dashed), and C3S NAT (purple solid). The x-axis represents the month of the year, and the y-axis indicates the percentage of hours. Lines correspond to the median values and the area between the first and third quartiles is shaded. Note the different y-axis scale for b).

487 due to its natural limitations, inevitably leading to higher reserve capacity
 488 needs during winter months as reliance on RES increases. Such insights are
 489 essential for policymakers to develop targeted strategies that enhance grid
 490 resilience and ensure a stable energy supply throughout the year.

491 5. Conclusions

492 This study has explored the characterisation of RES droughts in the real-
 493 life transition from a wind-dominated system to a more balanced system
 494 with integrated solar PV. This has been done through the comparison over
 495 a 45-year period of three different datasets: one based on a hand-crafted
 496 validated model and two based on a generic model, C3S-Energy. The generic
 497 model has two versions, one using large-scale aggregated information, and

one which includes the locations of farms as well (also considered in the validated model).

Our results show that generic datasets present limitations in the quantification of RES droughts. Although the three datasets used capture overall trends in drought occurrence, significant differences emerge when using non-tailored data for the study of RES droughts. This finding highlights that the choice of dataset and its underlying assumptions can lead to consequential differences in estimated RES drought characteristics, emphasising the need for datasets that are specifically designed for extreme event analysis.

This study reveals that differences in model parametrisation, particularly in the representation of wind turbine power curves and solar PV panel characteristics, have a stronger influence on the drought estimates than the inclusion of RES farm locations. The use of a validated dataset with a carefully selected wind turbine power curve consistently produced higher return periods and a greater number of drought events for wind energy than the datasets derived from C3S-Energy. This suggests that fine-tuning model parameters to match observed data is crucial for accurately quantifying RES drought risks, thereby supporting more effective energy system planning.

Finally, the effect on RES droughts of the integration of solar PV in a wind-dominated system has been explored in a real-case setting. In the presented example of Ireland, the analysis has demonstrated that transitioning to a more balanced system with similar amounts of wind and solar PV markedly reduces the frequency, duration, and seasonal variability of drought events. This improvement is attributed to the complementary nature of wind and solar PV generation, as solar PV typically peaks in summer while wind generation is more consistent in winter. Thus, a more diversified renewable energy mix not only mitigates extreme drought conditions but also enhances overall system resilience, providing valuable insights for policymakers tasked with ensuring energy security.

The results presented in this study have several limitations. Although ERA5 is among the best reanalysis datasets for renewable energy analysis, it still presents some biases, and its resolution may not capture local-scale phenomena. This is especially limiting if individual farms are considered, but it still shows good skill at statistically representing nation-wide behaviours considering the distribution of farms. Moreover, the methodology employs a fixed threshold to define RES drought events, which is necessary for comparing the three datasets considering only weather-derived drivers, but does not account for demand variations. Consequently, while this approach enables a

536 consistent inter-comparison, it will not signal events that are most critical for
537 power system operations for their mismatch of RES generation and demand.

538 Future work is planned to extend the current analysis. First, climate
539 projection data will be integrated with different energy scenarios, incorpo-
540 rating the addition of offshore wind, to better understand how climate change
541 might affect RES droughts. Second, expanding the geographic domain of the
542 study to include the rest of Europe would provide a more comprehensive un-
543 derstanding of RES droughts in an interconnected energy grid. This would
544 require extensive verification across other European countries, making it a
545 more complex but highly relevant challenge.

546 Data Availability

547 The ERA5 data can be obtained from the Climate Data Store (<https://doi.org/10.24381/cds.adbb2d47>). The C3S datasets are also available
548 from the Climate Data Store (<https://doi.org/10.24381/cds.4bd77450>).
549 Information on wind and solar PV farms in Ireland can be obtained from
550 the EirGrid website (<https://www.eirgrid.ie/grid/system-and-renewable-data-reports>). The Atlite model used in this study is open-source
551 and can be found on GitHub (<https://github.com/pypsa/atlite>). The
552 data and code required to reproduce the analysis in this article will be made
553 available upon acceptance of the manuscript in a public GitHub repository.

556 Acknowledgments

557 The research conducted in this publication was funded by Science Foun-
558 dation Ireland and co-funding partners under grant number 21/SPP/3756
559 through the NexSys Strategic Partnership Programme.

560 References

- 561 [1] EuroStat, Renewable Energy Statistics, 2023. URL: https://ec.europa.eu/eurostat/statistics-explained/index.php?title=Renewable_energy_statistics, Accessed: 2024-11-06.
- 562
563
564 [2] H. C. Bloomfield, D. J. Brayshaw, L. C. Shaffrey, P. J. Coker, H. E.
565 Thornton, Quantifying the increasing sensitivity of power systems to
566 climate variability, Environmental Research Letters 11 (2016) 124025.
567 doi:10.1088/1748-9326/11/12/124025.

- [3] H. C. Bloomfield, D. J. Brayshaw, A. Troccoli, C. M. Goodess, M. De Felice, L. Dubus, P. E. Bett, Y.-M. Saint-Drenan, Quantifying the sensitivity of european power systems to energy scenarios and climate change projections, *Renewable Energy* 164 (2021) 1062–1075. doi:10.1016/j.renene.2020.09.125.
- [4] F. Kaspar, M. Borsche, U. Pfeifroth, J. Trentmann, J. Drücke, P. Becker, A climatological assessment of balancing effects and shortfall risks of photovoltaics and wind energy in germany and europe, *Advances in Science and Research* 16 (2019) 119–128. doi:10.5194/asr-16-119-2019.
- [5] F. Mockert, C. M. Grams, T. Brown, F. Neumann, Meteorological conditions during periods of low wind speed and insolation in Germany: The role of weather regimes, *Meteorological Applications* 30 (2023) e2141. doi:10.1002/met.2141.
- [6] M. Ohba, Y. Kanno, D. Nohara, Climatology of dark doldrums in japan, *Renewable and Sustainable Energy Reviews* 155 (2022) 111927. doi:10.1016/j.rser.2021.111927.
- [7] M. J. Mayer, B. Biró, B. Szücs, A. Aszódi, Probabilistic modeling of future electricity systems with high renewable energy penetration using machine learning, *Applied Energy* 336 (2023) 120801. doi:10.1016/j.apenergy.2023.120801.
- [8] D. Raynaud, B. Hingray, B. François, J. Creutin, Energy droughts from variable renewable energy sources in European climates, *Renewable Energy* 125 (2018) 578–589. doi:https://doi.org/10.1016/j.renene.2018.02.130.
- [9] A. Gangopadhyay, A. K. Seshadri, N. J. Sparks, R. Toumi, The role of wind-solar hybrid plants in mitigating renewable energy-droughts, *Renewable Energy* 194 (2022) 926–937. doi:10.1016/j.renene.2022.05.122.
- [10] J. Kapica, J. Jurasz, F. A. Canales, H. Bloomfield, M. Guezgouz, M. De Felice, Z. Kobus, The potential impact of climate change on european renewable energy droughts, *Renewable and Sustainable Energy Reviews* 189 (2024) 114011. doi:10.1016/j.rser.2023.114011.

- [11] K. Z. Rinaldi, J. A. Dowling, T. H. Ruggles, K. Caldeira, N. S. Lewis, Wind and Solar Resource Droughts in California Highlight the Benefits of Long-Term Storage and Integration with the Western Interconnect, *Environmental Science and Technology* 55 (2021) 6214–6226. doi:10.1021/acs.est.0c07848.
- [12] P. T. Brown, D. J. Farnham, K. Caldeira, Meteorology and climatology of historical weekly wind and solar power resource droughts over western North America in ERA5, *SN Applied Sciences* 3 (2021) 814. doi:10.1007/s42452-021-04794-z.
- [13] S. Allen, N. Otero, Standardised indices to monitor energy droughts, *Renewable Energy* 217 (2023) 119206. doi:10.1016/j.renene.2023.119206.
- [14] C. Bracken, N. Voisin, C. D. Burleyson, A. M. Campbell, Z. J. Hou, D. Broman, Standardized benchmark of historical compound wind and solar energy droughts across the Continental United States, *Renewable Energy* 220 (2024) 119550. doi:https://doi.org/10.1016/j.renene.2023.119550.
- [15] H. Lei, P. Liu, Q. Cheng, H. Xu, W. Liu, Y. Zheng, X. Chen, Y. Zhou, Frequency, duration, severity of energy drought and its propagation in hydro-wind-photovoltaic complementary systems, *Renewable Energy* (2024) 120845. doi:10.1016/j.renene.2024.120845, 2.
- [16] H. Hersbach, B. Bell, P. Berrisford, S. Hirahara, A. Horányi, J. Muñoz-Sabater, J. Nicolas, C. Peubey, R. Radu, D. Schepers, et al., The ERA5 global reanalysis, *Quarterly Journal of the Royal Meteorological Society* 146 (2020) 1999–2049. doi:10.1002/qj.3803.
- [17] L. Dubus, Y. Saint-Drenan, A. Troccoli, M. De Felice, Y. Moreau, L. Ho-Tran, C. Goodess, R. Amaro E Silva, L. Sanger, C3S Energy: A climate service for the provision of power supply and demand indicators for Europe based on the ERA5 reanalysis and ENTSO-E data, *Meteorological Applications* 30 (2023) e2145. doi:10.1002/met.2145.
- [18] F. Hofmann, J. Hampp, F. Neumann, T. Brown, J. Hörsch, Atlite: a lightweight Python package for calculating renewable power potentials

633 and time series, *Journal of Open Source Software* 6 (2021) 3294. doi:10
634 .21105/joss.03294.

635 [19] A. Kies, B. U. Schyska, M. Bilousova, O. El Sayed, J. Jurasz,
636 H. Stoecker, Critical review of renewable generation datasets and their
637 implications for european power system models, *Renewable and Sus-
638 tainable Energy Reviews* 152 (2021) 111614. doi:10.1016/j.rser.202
639 1.111614.

640 [20] EirGrid & SONI, System and Renewable Data Reports, 2023. URL:
641 [https://www.eirgrid.ie/grid/system-and-renewable-data-rep
642 orts](https://www.eirgrid.ie/grid/system-and-renewable-data-reports), Accessed: 2024-11-06.

643 [21] Y.-M. Saint-Drenan, L. Wald, T. Ranchin, L. Dubus, A. Troccoli, An
644 approach for the estimation of the aggregated photovoltaic power gener-
645 ated in several European countries from meteorological data, *Advances
646 in Science and Research* 15 (2018) 51–62. doi:10.5194/asr-15-51-201
647 8.

648 [22] I. Staffell, S. Pfenninger, Using bias-corrected reanalysis to simulate
649 current and future wind power output, *Energy* 114 (2016) 1224–1239.
650 doi:10.1016/j.energy.2016.08.068.

651 [23] Government of Ireland, Climate Action Plan 2024, Technical Report 3,
652 Department of the Environment, Climate and Communications, 2023.
653 URL: [https://www.gov.ie/pdf/?file=https://assets.gov.ie/
654 284675/70922dc5-1480-4c2e-830e-295afd0b5356.pdf](https://www.gov.ie/pdf/?file=https://assets.gov.ie/284675/70922dc5-1480-4c2e-830e-295afd0b5356.pdf), Accessed:
655 2024-11-06.

656 [24] Sustainable Energy Authority Ireland, National Energy Projections
657 2024, Technical Report, Sustainability Energy Authority of Ireland,
658 2024. URL: [https://www.seai.ie/news-and-events/news/energ
659 y-projections-report](https://www.seai.ie/news-and-events/news/energy-projections-report), Accessed: 2024-11-06.

660 [25] H. G. Beyer, G. Heilscher, S. Bofinger, A robust model for the mpp
661 performance of different types of pv-modules applied for the performance
662 check of grid connected systems, *Eurosun* (2004) 8.